Journal of Magnetic Resonance **138,** 320–325 (1999)
Article ID jmre.1999.1739, available online at http://www.idealibrary.com on IDEAL®

Multiple-Rotor-Cycle QPASS Pulse Sequences: Separation of Quadrupolar Spinning Sidebands with an Application to ^{139}La NMR

David J. Aurentz,[1] Frederick G. Vogt, Karl T. Mueller, and Alan J. Benesi[2]

Department of Chemistry, Pennsylvania State University, 152 Davey Laboratory, University Park, Pennsylvania 16802-6300

Received September 9, 1998; revised February 17, 1999

The quadrupolar phase-adjusted spinning sidebands (QPASS) pulse sequence has been recently demonstrated as a useful method for obtaining quadrupolar parameters with magic-angle spinning NMR. The sequence separates spinning sidebands by order in a two-dimensional experiment. A sheared projection of the 2D spectrum effectively yields the infinite spinning rate second-order quadrupolar powder pattern, which can be analyzed to determine quadrupolar coupling constants and asymmetry parameters. The RF power and spinning speed requirements of the original QPASS sequence make it an experimentally demanding technique. A new version of the sequence is demonstrated here and is shown to alleviate many problems associated with the original sequence. New solutions to the determining equations, based on the use of multiple rotor cycles in the QPASS sequence, lead to longer delays between the nine π pulses, provide less chance of pulse overlap, and allow for use of weaker RF field strengths that excite only the central quadrupolar transition. A three-rotor-cycle version of the new experiment is demonstrated on the ^{139}La nucleus. © 1999 Academic Press

Key Words: **QPASS; sideband separation; second-order quadrupolar interaction; lanthanum-139.**

Spinning sidebands present in magic-angle spinning (MAS) NMR (*1*, *2*) spectra of spin-$\frac{1}{2}$ nuclei can make the interpretation of isotropic chemical shifts difficult due to sideband overlap and the attenuation of the isotropic peak intensities. Sidebands can be eliminated from spectra by utilizing low magnetic fields or by spinning the sample at a rate greater than the width of frequencies produced by the chemical-shift anisotropy (CSA). However, the loss of the sidebands decreases the chemical-shift information content due to the second-rank tensor nature of the CSA (*3*). Procedures for separating the isotropic and anisotropic chemical-shift interactions while retaining their information have been demonstrated in the phase-adjusted spinning sidebands experiment (PASS) (*4*) and the 2D PASS experiment (*5*). In the latter, spinning-sideband manifolds are separated by order into a 2D array of spectra through the manipulation of five π pulses during a fixed duration of one rotor period.

For half-integer quadrupoles, spectra are further complicated by second-order anisotropic quadrupolar interactions that are not sufficiently suppressed by the motional averaging of MAS (*6*). Nuclei with large quadrupolar coupling constants ($C_Q = e^2qQ/h$) are particularly difficult to analyze using MAS because even at very high spinning rates (i.e., 20–30 kHz), the second-order broadened sidebands still overlap, yielding highly distorted spectra containing very little interpretable information about the quadrupolar interaction. Clean isolation of spinning sidebands from the isotropic resonance for powdered samples undergoing magic-angle spinning and subjected to pure second-order quadrupolar Hamiltonians has recently been achieved by the quadrupolar PASS (QPASS) pulse sequence (*7*). This method of sideband separation is analogous in design to the 2D PASS sequence, but is based on the modulation of sideband order using nine π pulses spaced within a one-rotor-cycle evolution period. As noted by Massiot *et al.* (*7*), high spinning rates are desirable for this technique, leading to short rotor periods and insufficient delays between the nine finite π pulses.

The goal of this communication is to present an interpretation of the QPASS experiment which facilitates its application at high spinning speeds. There are two ways in which this is accomplished. The first is the extension of the sequence from a single rotor cycle to multiple rotor cycles. The second is the selection of sets of timing delays for the nine π pulses which are solutions to the QPASS equations, but are spread as evenly from one another as permitted by the pitch angle condition. Application of a new multiple rotor-cycle QPASS sequence to a sample of $LaCl_3$ is also presented as an example of the potentially useful information that can be obtained from the ^{139}La nucleus. This nucleus is of chemical interest because of its use in catalytic systems.

The theoretical basis for the separation of spinning sidebands by their order (k) has been well described in previous work (*4*, *8*). Although the spinning sidebands in routinely published spectra display a uniform phase (*9*), an appropriate pulse sequence can shift sideband phases by $-k\Theta$, where Θ is the pitch angle associated with sets of delays between π pulses

[1] Present address: Air Products and Chemicals, 7201 Hamilton Blvd., Allentown, PA 18195-1501.

[2] To whom correspondence should be addressed.

1090-7807/99 $30.00

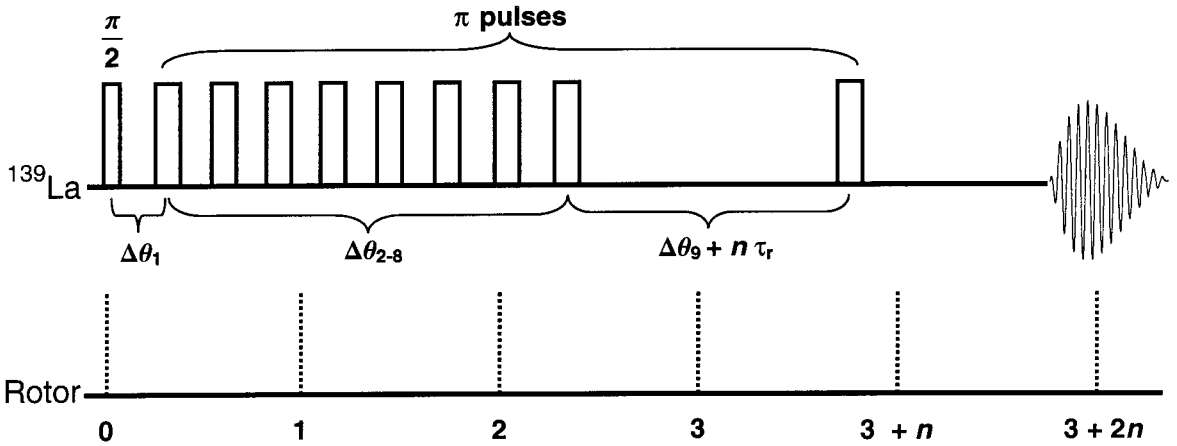

FIG. 1. The three-rotor-cycle QPASS pulse sequence used in this work. Shifted-echo detection is utilized, and n is usually set to 1. The π pulses and the receiver are independently phase cycled as discussed in the text.

(*4*). Clean sideband separation for powdered samples undergoing MAS and subject to first and second-order Hamiltonians can be achieved by satisfying the PASS equations (*5*):

$$2\sum_{q=1}^{n}(-1)^q\exp(im\theta_q) + 1 - (-1)^n\exp(im(\Theta + \theta_T)) = 0 \quad [1]$$

$$-2\sum_{q=1}^{n}(-1)^{n+q}\theta_q + \theta_T = 0, \quad [2]$$

where n is the number of π pulses in the sequence, $\theta_q = \omega_r\tau_q$ (where ω_r is the MAS rotor frequency in radians per second and τ_q is the time delay in seconds to the center of the qth π pulse in relation to the beginning of the evolution period) and $\theta_T = \omega_r T$ (where T is the total duration of the evolution period). In the case of QPASS, nine nonlinear equations (five real and four imaginary) for $m = 1$ to 4 are solved for the unknown delays, θ_q, of the nine pulses ($n = 9$) over a fixed θ_T. In the previous work, the QPASS equations were solved only for $\theta_T = 2\pi$ (one rotor cycle) and code to generate the delay tables was presented (*7*). All time values were calculated using fixed starting points for a Newton–Raphson root-finding algorithm (*10*), thereby generating a unique set of solutions at each pitch. The equations also allow for multiple rotor-cycle solutions, a three-rotor-cycle version of which is pictured in Fig. 1. Multiple rotor-cycle solutions greatly increase the amount of time available to apply the nine finite π pulses. However, unlike the single-rotor-cycle solutions, the QPASS solutions for a given Θ are not unique for multiple-rotor-cycle evolution periods (e.g., $\theta_T = 6\pi$ and 10π). Use of a random number generator to provide the starting values for the Newton–Raphson method gives rise to many different sets of θ_q solutions for each Θ value. This aspect of multiple rotor period evolution provides another option to help relieve the congestion of π pulses in a single QPASS rotor period. Sets of solutions may be screened until delays with the maximum possible time between pulses ($\Delta\tau_q$) are found. In our computations, we have found that well-spaced solutions can be found for three- and five-rotor-cycle QPASS. At the present time, no numerical solutions could be obtained for two- and four-rotor-cycle QPASS, and only the previously published solution (*7*) was obtainable for one-rotor-cycle QPASS. While this does not constitute proof that no additional solutions are available for these problems, it appears that this is the case, as many days of computer search time were expended on this issue. The calculation of sets of delays for both three- and five-rotor-cycle QPASS experiments can been achieved using Mathematica code (*18*), which solves the QPASS equations by the Newton–Raphson method. The solution process is started via a random number generator with a limited range of 2π centered around the delays for $\Theta = 0$. One particularly well-optimized set of solutions for a three-rotor-cycle experiment is given in Table 1, the values of which were found by enforcing an empirical maximization of the spacing between pitch angles ($\Delta\theta_q$). In Table 1, the QPASS solutions are listed for all θ_q's corresponding to 16 pitch angles from 0 to 2π. A plot of the pitch angle versus the timing of delays for these values is shown in Fig. 2, where the relatively even distribution of pulse delays throughout the sequence is easily visualized.

All ^{139}La spectra were obtained on a Chemagnetics/Varian Infinity 11.74 T spectrometer operating at a spectral frequency of 70.564206 MHz using a 5-mm double-resonance Chemagnetics probe (Model MPRB 500318). Spinning during the QPASS experiment was locked at 10 kHz $\pm$ 2 Hz via a Chemagnetics MAS Speed Controller (Model M806403000) to ensure a reproducible rotor cycle which is critical to the success of the fixed duration QPASS timing period. A low RF

TABLE 1
Timings for π Pulses, Given as Sample Revolution Angles (in Radians), for Three Rotor-Cycle QPASS

Pitch ($\Theta/2\pi$)	$\theta_1/2\pi$	$\theta_2/2\pi$	$\theta_3/2\pi$	$\theta_4/2\pi$	$\theta_5/2\pi$	$\theta_6/2\pi$	$\theta_7/2\pi$	$\theta_8/2\pi$	$\theta_9/2\pi$ [a]
0.0000	0.30000	0.60000	0.90000	1.20000	1.50000	1.80000	2.10000	2.40000	2.70000
0.0625	0.32536	0.62995	0.91992	1.23260	1.52420	1.82840	2.12920	2.43090	2.72310
0.1250	0.34714	0.65297	0.92846	1.26330	1.54260	1.84720	2.16360	2.45680	2.73850
0.1875	0.35132	0.65836	0.92425	1.27700	1.54320	1.85010	2.19440	2.46460	2.73690
0.2500	0.32855	0.64778	0.91278	1.24230	1.52500	1.84230	2.19620	2.45130	2.72120
0.3125	0.33595	0.64528	0.90391	1.20070	1.51780	1.83900	2.16700	2.45190	2.71220
0.3750	0.35594	0.63867	0.89374	1.19010	1.50400	1.83390	2.15180	2.44260	2.69990
0.4375	0.34658	0.62983	0.88271	1.18430	1.48580	1.82780	2.14010	2.39890	2.68580
0.5000	0.32390	0.62708	0.87292	1.17610	1.50000	1.82390	2.12710	2.37290	2.67610
0.5625	0.31424	0.60111	0.85993	1.17220	1.51420	1.81570	2.11730	2.37020	2.65340
0.6250	0.30009	0.55736	0.84823	1.16610	1.49600	1.80990	2.10630	2.36130	2.64410
0.6875	0.28780	0.54813	0.83300	1.16100	1.48220	1.79930	2.09610	2.35470	2.66410
0.7500	0.27878	0.54867	0.80385	1.15770	1.47500	1.75770	2.08720	2.35220	2.67150
0.8125	0.26308	0.53539	0.80563	1.14990	1.45680	1.72300	2.07580	2.34160	2.64870
0.8750	0.26147	0.54319	0.83644	1.15280	1.45740	1.73670	2.07150	2.34700	2.65290
0.9375	0.27686	0.56905	0.87082	1.17160	1.47580	1.76740	2.08010	2.37000	2.67460

[a] For shifted-echo detection, one or more additional rotor cycles can be inserted prior to and after this delay, as in Fig. 1.

field strength was employed to deliver the π pulses of length 5.7 μs throughout the QPASS evolution. The sequence was run in a hypercomplex format (*11*, *12*) to help compensate for artifacts that occur along the k dimension and shifted-echo detection (*7*) was utilized in order to ensure acquisition of the echo maximum. Independent phase cycling of the nine π pulses in steps of $2\pi/3$, and appropriate adjustment of the receiver phase, was employed to select an alternating $(+1) \rightarrow (-1) \rightarrow (+1) \rightarrow (\cdots)$ coherence pathway (*5*).

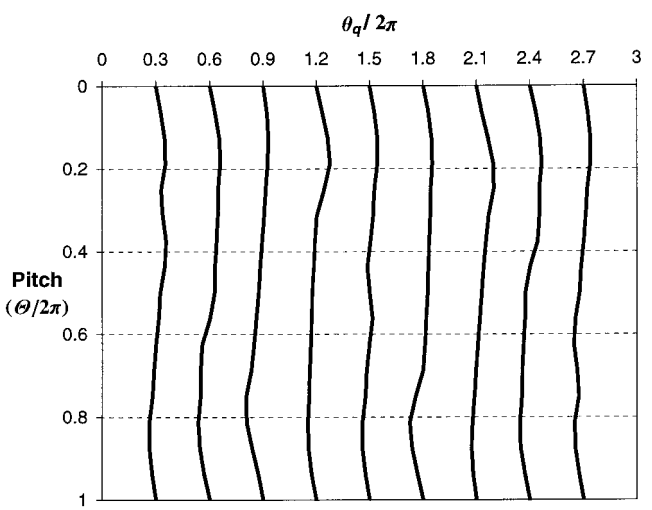

FIG. 2. Timings for the nine π pulses in the three-rotor-cycle QPASS sequence, in units of sample revolution angle, plotted as a function of pitch angle. All angles are in radians. Note that the wider spacing between the lines (and thus the π pulses) compared to the one-rotor-cycle QPASS sequence lessens the RF power requirements (see text).

Static spectra were recorded by using a $\{\theta$–τ_1–2θ–τ_2–Acquire$\}$ echo experiment, where θ is the tip angle of the pulse (*13*), with a θ pulse duration of 3.5 μs, a τ_1 echo delay of 35 μs, and a τ_2 echo delay of 30 μs. The phase cycle for the θ pulse was $\{x, -x, y, -y\}$ and for the 2θ pulse was $\{y, y, -x, -x\}$. The receiver was phase cycled in the same manner as the θ pulse.

The result of a ^{139}La three-rotor-cycle hypercomplex QPASS experiment on lanthanum chloride, $LaCl_3$ (Aldrich Chemical Co.), is shown in Fig. 3. $LaCl_3$ was chosen as a test compound primarily because of its close relation to other chemically interesting lanthanum compounds, but also because ^{139}La has a high natural abundance (99.9%), is extremely sensitive to the effects of changes in local electric field gradients (EFGs), and exhibits wide linewidths due to strong quadrupolar interactions. The quadrupolar parameters for ^{139}La ($I = \frac{7}{2}$) of a single crystal of anhydrous $LaCl_3$ have been reported previously (*14*). The quadrupolar coupling constant (C_Q) is 15.3 MHz and the asymmetry parameter (η) is equal to zero indicating axial symmetry.

The stacked 2D plot in Fig. 3 retains the MAS-averaged second-order quadrupolar interaction in the ω_2 dimension, but separates the spinning sidebands by their order, k, in the ω_1 dimension. Due to the combination of fast (10 kHz) MAS and the 15.3-MHz quadrupolar coupling constant, only 16 pitches are required to achieve sideband separation, thus shortening the experimental time to a total of 12 h. Shearing of the appropriate

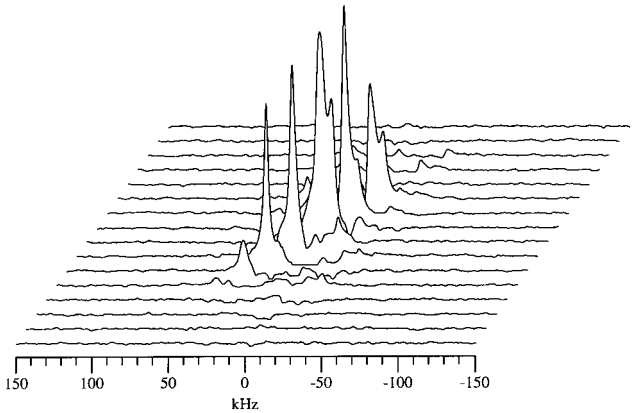

FIG. 3. The 2D, 16-pitch angle QPASS spectrum obtained from the $LaCl_3$ sample, spinning at a MAS speed of 10 kHz. At least six separated sidebands are visible. The data shown were acquired in hypercomplex mode, with a total experimental time of 12 h (see text).

sidebands (*15*) yields the *infinite spinning rate* spectrum presented in Fig. 4d. This infinite spinning rate spectrum provides more accurate information about the EFG than the static pattern which contains CSA and dipolar interactions. These anisotropic first-order interactions are removed in the sheared QPASS spectrum, leaving only the equivalent of the second-order infinite spinning rate MAS spectrum. The second-order quadrupolar lineshape can be fit directly with only the quadrupolar parameters as shown by the simulated second-order pattern in Fig. 4b (*7*), which matches the experimental data based on the position of the singularities and the overall width of the pattern.

The experimental static $LaCl_3$ pattern displayed in Fig. 4c contains a small amount of additional intensity on either side of the $\eta = 0$ pattern as well as a bump in the center of the pattern when compared to a simulated static pattern in Fig. 4a. Small amounts of water are known to readily replace the Cl^- ions in $LaCl_3$ with OH^- and O^{2-} (*16*). The $LaCl_3$ sample used in the QPASS and static experiments was heated at 750°C for 2 h in an attempt to remove all water but the presence of a second La site of higher η is indicated in both the static and the infinite spinning rate spectrum. Other less plausible explanations for the nonideality of these lineshapes include nonuniform T_2 relaxation, differential excitation of multiple quantum coherences, and nonuniform RF excitation across the powder pattern. However, since the principal features of the powder patterns are not significantly affected, this does not affect the analysis of the quadrupolar parameters for this sample. The ability of water molecules to modify the EFG tensor in $LaCl_3$ has been reported previously (*14*), in a study of pure $LaCl_3 \cdot$ ca. $6H_2O$, which has a C_Q of 23.7 MHz and an η of 0.4. The strong effect of water demonstrates the sensitivity of the ^{139}La nucleus to chemical modification.

The extreme width of the static second-order quadrupolar pattern associated with large C_Q's makes the use of fast spinning rates necessary, in order to reduce both the number of

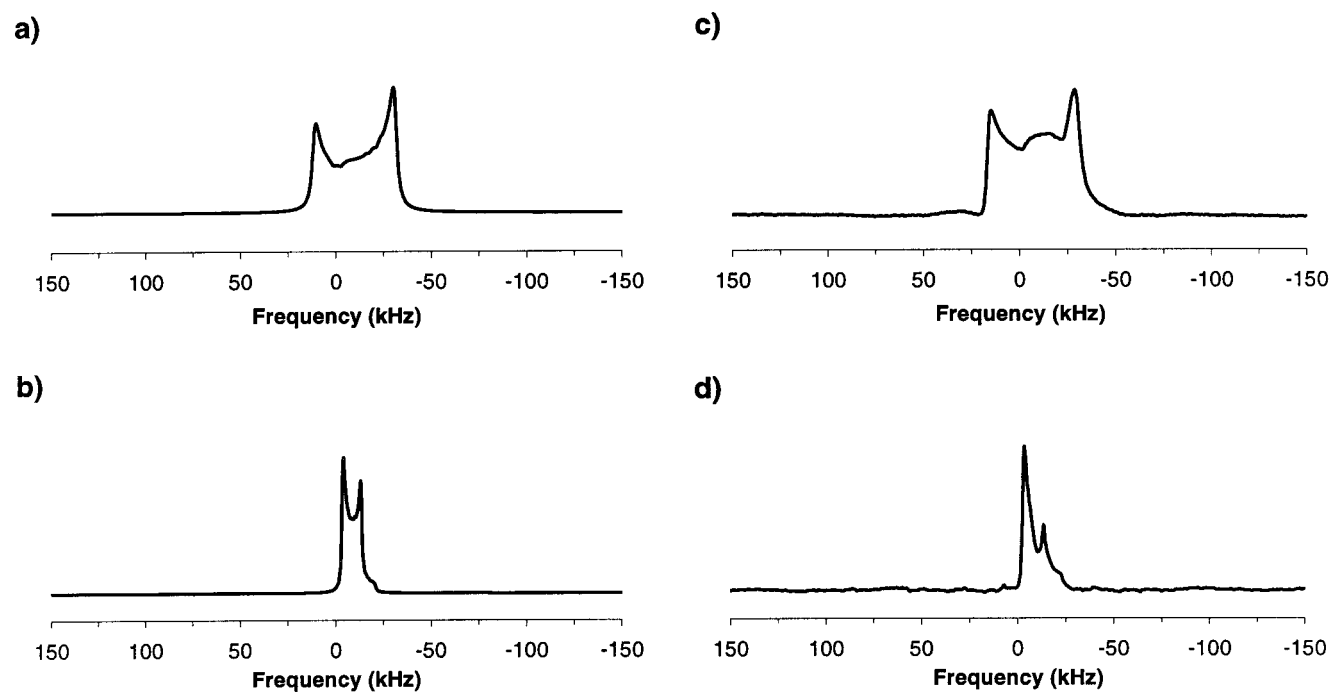

FIG. 4. (a) Simulated static $LaCl_3$ spectrum, with a C_Q of 15.3 MHz and an η equal to zero. (b) Simulated infinite spinning rate MAS spectrum of $LaCl_3$. (c) Experimental static echo spectrum of $LaCl_3$ (see text). (d) Infinite spinning rate spectrum obtained by shearing the $LaCl_3$ QPASS data shown in Fig. 3.

possible sidebands and the duration of the 2D experiment. The correspondingly short length of one rotor cycle dictates a fixed duration evolution period, which makes application of nine π pulses extremely demanding if feasible at all. The addition of multiple rotor cycles to the evolution period not only makes the application of QPASS to nuclei with high C_Q values possible, but the extra time afforded by several rotor cycles provides more flexibility in RF field strengths. In order to remain in the soft pulse regime for nuclei with moderate to small C_Q's, the RF field strength must be much less than the quadrupolar frequency (*17*). This condition is desirable to avoid exciting transitions other than the central transition for half-integer quadrupoles and can be achieved through the use of longer $\pi/2$ and π pulse lengths. A low RF power was utilized in these experiments so that only the central transition of the ^{139}La resonance was excited. This was intended to alleviate the stress on the phase cycle by minimizing the excitation of multiple-quantum coherences. We have found experimentally that the low RF powers employed in this work aid in the suppression of spectral artifacts (possibly due to multiple-quantum effects), while their effects on the central transition can be negated via a first-order phase correction. The limited excitation bandwidth provided by this RF power may have contributed to the non-ideal shape of the sheared QPASS spectrum, although the additional site visible in the static spectrum is probably the main cause.

As previously mentioned, multiple solutions are possible for the pulse timings in multiple-rotor-cycle QPASS. Solutions can be chosen that maximize the delays between adjacent π pulses. Delays such as those shown in Table 1 and Fig. 2 eliminate the narrow spacing between pulses generated by the unique solutions to the QPASS equations for a single-rotor-cycle experiment. The shortest maximum $\Delta\theta_q$ calculated for the set of QPASS delays in Table 1 is 8.2% of three rotor periods, compared to the 4.4% of one rotor period in the original one-rotor-cycle QPASS. A practical guide for determining the feasibility of the delays in a QPASS experiment is to take the actual time of the shortest delay and compare it to the instrumental limit of the spectrometer:

$$N\tau_r\delta - t_\pi > \text{instrumental limit}, \qquad [3]$$

where N is the number of rotor cycles, τ_r is the rotor period, δ is the minimum $\Delta\theta_q$ fraction, and t_π is the length of the π pulse. In the case of our three-rotor-cycle experiment, the shortest delay is 18.9 μs (i.e., $3 \times 100\ \mu\text{s} \times 0.082 - 5.7\ \mu\text{s}$), which is much greater than instrumental limits in the range of 0.1 to 0.5 μs. In more severe cases, the use of a five-rotor-cycle QPASS sequence might be warranted. This subject is under investigation.

A drawback to the addition of more rotor periods to the QPASS is decreased signal intensity from transverse relaxation during the increased evolution time. However, this effect is minimized by the rapid sample rotation in this experiment, and, in practice, transverse relaxation is not a significant problem.

It is also important to note that the same approach can be incorporated into the 2D PASS sequence to aid in the acquisition of sideband-separated spectra of spin-$\frac{1}{2}$ nuclei. We have calculated optimal PASS delays for two- and three-rotor-cycle experiments by solving the five nonlinear equations (three real and two imaginary) for the five unknowns produced by Eqs. [1] and [2]. An interesting trait of both *single* rotor period 2D PASS and QPASS experiments is that there exists only one set of θ_q solutions to the nonlinear equations. Attempting to find other solutions through the use of the random starting points for Newton's method always returned the same solutions, which exactly match those of Refs. (*5*) and (*7*).

In conclusion, a three-rotor-cycle QPASS experiment has been successfully performed on a $LaCl_3$ sample allowing the separation of overlapping sidebands and the determination of quadrupolar parameters in agreement with previous results. The expansion of the QPASS experiment to multiple rotor cycles avoids the experimental difficulty of including nine pulses and 10 delays within a single rotor period. This advantage is especially useful for quadrupolar nuclei with large quadrupolar coupling constants where rapid sample rotation and correspondingly short rotor periods are a necessity. An optimized set of solutions to the QPASS equations with $n = 9$ and a fixed overall delay period (θ_T) of three rotor cycles (6π) has been presented here.

We have introduced this augmentation of the original QPASS experiment with ^{139}La spectra of $LaCl_3$ and anticipate its application to other materials where the sensitivity of ^{139}La to the EFG can be used to probe chemically interesting structures. An important example is that of the reduction of NO_x gases by methane over La_2O_3 (*19*). Furthermore, decreasing the experimental challenges involved with the QPASS experiment should help promote its use with other nuclei where overlapping sideband intensities have made analysis of quadrupolar parameters difficult.

ACKNOWLEDGMENTS

This report is based upon work supported by the National Science Foundation under Grant DMR-9458053. Support was also provided by the Research Corporation (Cottrell Scholars Program). The NMR spectrometer used in this work was obtained through the assistance of the National Science Foundation under Grant CHE-9601572. Prof. Dominique Massiot and Dr. Cindy Ridenour (Chemagnetics/Varian) are thanked for helpful discussions.

REFERENCES

1. E. R. Andrew, A. Bradbury, and R. G. Eades, *Nature* **183,** 1802 (1959).
2. I. J. Lowe, *Phys. Rev. Lett.* **2,** 285 (1959).
3. J. Herzfeld and A. E. Berger, *J. Chem. Phys.* **73,** 6021 (1980).
4. W. T. Dixon, *J. Chem. Phys.* **77,** 1800 (1982).

5. O. N. Antzutkin, S. C. Shekar, and M. H. Levitt, *J. Magn. Reson. A* **115,** 7 (1995).
6. A. Samoson, E. Kundla, and E. Lippmaa, *J. Magn. Reson.* **49,** 350 (1982).
7. D. Massiot, V. Montouillout, F. Fayon, P. Florian, and C. Bessada, *Chem. Phys. Lett.* **272,** 295 (1997).
8. W. T. Dixon, *J. Magn. Reson.* **44,** 220 (1981).
9. M. H. Levitt, *J. Magn. Reson.* **82,** 427 (1989).
10. W. H. Press, B. P. Flannery, S. A. Teukolsky, and W. T. Vetterling, "Numerical Recipes in Fortran," 2nd ed., Cambridge Univ. Press, London (1995).
11. J. Keeler, *J. Magn. Reson.* **63,** 454 (1985).
12. D. J. States, R. A. Haberkorn, and D. J. Ruben, *J. Magn. Reson.* **48,** 286 (1982).
13. D. Freude and J. Haase, *in* "NMR Basic Principles and Progress," Vol. 29, Springer-Verlag, Berlin (1993).
14. B. Herreros, P. P. Man, J. M. Manoli, and J. Fraissard, *J. Chem. Soc. Chem. Commun.* **6,** 464 (1992).
15. R. R. Ernst, G. Bodenhausen, and A. Wokaun, "Principles of Nuclear Magnetic Resonance in One and Two Dimensions," p. 610, Clarendon Press. Oxford (1987).
16. D. V. Ormondt, R. D. Beer, C. M. D. Jong, M. G. V. D. Oord, M. H. Homs, and H. W. D. Hartog, *Physica B* **84,** 110 (1976).
17. A. Samoson and E. Lippmaa, *J. Magn. Reson.* **79,** 255 (1988).
18. S. Wolfram, "Mathematica: A System for Doing Mathematics by Computer," Addison–Wesley, Reading, MA (1996).
19. X. Zhang, A. B. Walters, and M. A. Vannice, *Appl. Catal. B* **4,** 237 (1994).